

Evaluating the Effect of Filter Pre-processing on T1-Weighted MRI Images for Brain Tissue Segmentation

Justin T. Pontalba

*Faculty of Biomedical Engineering
Yeats School of Graduate Studies, Ryerson University
Toronto, Canada
jpontalb@ryerson.ca*

Abstract—MR Images are important for the diagnosis and management of neurological diseases. Automatic segmentation of brain tissues leverages the opportunity to reduce error and variability related to manual segmentation by medical practitioners. However, automatic segmentation is impacted by noise in MR images. This paper evaluates the effect of several pre-processing techniques on brain tissue segmentation using k-means clustering. The paper found that median filtering prior to segmentation resulted in the greatest segmentation accuracy with 0.755, 0.614, and 0.777 for white matter, grey matter, and cerebrospinal fluid respectively. Combining filter pipelines rather than using single filters, and using a more flexible segmentation method may lead to improved results.

Index Terms—Segmentation, White Matter, Grey Matter, Cerebrospinal Fluid, magnetic resonance imaging, T1-Weighted

I. INTRODUCTION

Neurological images are important for the diagnoses, prognoses, and management of neurological diseases. Health care providers, such as radiologists, use medical images for the diagnoses and treatment of disease or injury. Computed tomography (CT), single positron emission computed tomography (SPECT), magnetic resonance imaging (MRI), and ultrasound are just a few examples of imaging techniques used for disease diagnosis and prognosis. For neurological diseases, CT and MRI systems are common modalities to visualize the macroanatomy of the brain for suspected pathology. While both modalities can be used to visualize neurological disease, MRI images provide great detail for structures such as white matter (WM), grey matter (GM), cerebrospinal fluid (CSF), and pathology [1]. WM, GM, and CSF, regions can be analyzed by a radiologist for irregularities. However, factors such as fatigue, the multicenter effect (MCE), and inter- and intra-observer variability, negatively impact the manual analysis of these regions and thereby impact quality health care delivery.

Automated analysis of WM, GM, and CSF regions have been implemented to combat the variability encountered in the manual process [1] [2]. Methods such as fuzzy c-means, k-means clustering, and self-organized maps, are some examples of un-supervised methods for tissue segmentation. However, automated analysis is impacted by noise and acquisition

factors such as system manufacture, number of slices, slice thickness, voxel resolution, and bias field artefacts [3].

In this paper, brain tissue segmentation using k-means clustering is analyzed with respect to various filters used for pre-processing. For this paper, only pre-processing methods for additive noise are addressed. Specifically, segmentation performance is analyzed with respect to additive noise levels, slice thickness, and the applied pre-processing method.

The paper is organized as follows: Section II describes the methods of pre-processing and segmentation. Section III outlines the results of the experiments, and Section IV contains some final remarks and suggests future work.

II. MATERIALS AND METHODS

A. Data

The data used in this paper are of five T1-weighted MRI volumes varied by slice thickness (1mm, 3mm, 5mm, 7mm, and 9mm) and additive Rician noise (0%, 1%, 3%, 5%, 7%, and 9%). In total, there are 30 volumes, where each volume is of a single slice thickness and additive noise level. Volumes in this dataset contain 20% and 40% bias field levels. Furthermore, each slice dimension is 181 x 217 pixels. Each volume has a corresponding label volume of binary WM, GM, and CSF labels. This paper analyzes how such properties affect pre-processing techniques in the application of brain tissue segmentation.

B. Experimental Design

The proposed experimental design is depicted in **Figure 1**. First, filtering is applied on a *slice-by-slice* basis using one of three different filtering methods, gaussian, median, or wiener filters. Next, the *skull stripping* is applied to extract the brain tissue region. *K-means clustering* is then used to segment various regions of brain. Finally, the centroids are assigned to the associated brain tissue label, and accuracy for segmentation is quantified.

C. Pre-processing Using Filters

1) *Gaussian Filter*: Gaussian noise and impulse noise are common noises distributed in magnitude MR images [4].

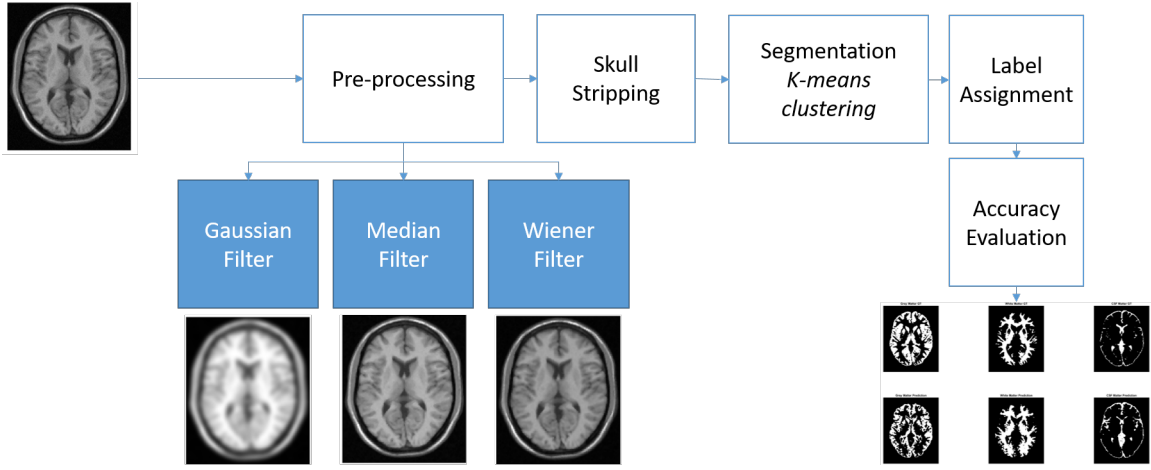


Fig. 1. Experimental design

Gaussian noise has a probability density equation that of a normal distribution, and is amplified or added during acquisition [5]. As such, a gaussian filter was chosen as a method for pre-processing. However, to avoid exhaustive approaches for tuning the σ of the filter, a noise estimation method by [5]. [5] methodology assumes additive zero mean Gaussian noise. [5] first apply first-order gradients for edge detection to exclude structures or details contributing to the noise variance estimation. Next, a Laplacian operator, followed by averaging is used to provide accurate noise variance estimation. [5] methodology assumes an imaging model with additive noise by

$$I_n = I(x, y) + n(x, y) \quad (1)$$

where x and y are the coordinates of the pixel and I_n , $I(x, y)$, and $n(x, y)$ are the noisy image, the original image, and the additive Gaussian noise respectively [5]. Returned by [5]’s algorithm is the estimated σ . σ is estimated on a slice-by-slice basis where σ is used to generate the associated Gaussian filter to be applied.

2) *Median Filter*: As an alternative method to filter the MR images, the median filter was applied prior to segmentation. The median filter is a spatial filter which replaces the center pixel of a given neighbourhood with the median of such neighbourhood. This filter was chosen for its capability to filter impulse and salt and pepper noise, and maintain structural similarity to that of the un-filtered image [4]. However, when applying the median filter, the neighbourhood size is a parameter that must be considered. Dimensions of the median filter dictate the locality of the result. Smaller kernel dimensions result in more localized filtering, whereas, large kernel dimensions result in more global effects [6]. To choose the ideal neighbourhood size, the neighbourhood size is varied and metrics such as *signal-to-noise ratio (SNR)*, *peak-signal-to-noise ratio (PSNR)*, and *structural similarity index (SSIM)* are used to quantify the comparison between the un-filtered image and the filtered image.

3) *Wiener Filter*: The Wiener filter was chosen to filter the MR images for its ability to filter noise. The wiener filter is an adaptive filter which employs a statistical approach. The filter assumes the signal and noise contained in the image are both linear stochastic processes with known spectral properties [7]. The goal of the filtering process is to minimize the mean squared error in the process of inverse filtering and noise smoothing [7]. The result of Wiener filtering is a linear estimation of the original image. Filtering is implemented in the frequency domain as follows:

$$W(f_1, f_2) = \frac{H(f_1, f_2)S_{xx}(f_1, f_2)}{\|H(f_1, f_2)\|^2 S_{xx}(f_1, f_2) + S_{nn}(f_1, f_2)} \quad (2)$$

where $S_{xx}(f_1, f_2)$ and $S_{nn}(f_1, f_2)$ are the power spectra of the original image and the additive noise, and $H(f_1, f_2)$ is the blurring filter. The Wiener filter has a two part methodology, i) inverse filtering and ii) noise smoothing. This apply high-pass and low-pass filtering respectively [7].

In this implementation, the Wiener filter is also dependent on neighbourhood size. Therefore, the same optimization methodology and validation metrics are used as in optimizing the neighbourhood size for the median filter.

D. Pre-processing Validation Metrics

To quantify the performance of the filters, signal-to-noise ratio, peak signal-to-noise ratio, and structural similarity index are used to compare the original image with the filtered image. These metrics are calculated on a slice-by-slice basis.

1) *Signal-to-noise ratio*: The SNR is defined in the spatial domain as:

$$SNR = 10 \log_{10} \left(\frac{\sum_{x=0}^{M-1} \sum_{y=0}^{N-1} \hat{f}(x, y)^2}{\sum_{x=0}^{M-1} \sum_{y=0}^{N-1} [f(x, y) - \hat{f}(x, y)]^2} \right) \quad (3)$$

where $f(x, y)$ is the original image and $\hat{f}(x, y)$ is the filtered image. The closer f and \hat{f} are, the larger the ratio will be. Preferred results would demonstrate a high SNR [6].

2) *Peak signal-to-noise ratio*: The PSNR is defined in the spatial domain as:

$$PSNR = 10 \log_{10} \left(\frac{\max(f(x, y))}{\sum_{x=0}^{M-1} \sum_{y=0}^{N-1} [f(x, y) - \hat{f}(x, y)]^2} \right) \quad (4)$$

where $f(x, y)$ is the original image and $\hat{f}(x, y)$ is the filtered image. Different from the SNR, the PSNR represents the ratio of the maximum intensity to the mean squared error between the original image and the filtered image. Preferred results would demonstrate a high PSNR [6].

3) *structural similarity index*: The SSIM is a quality assessment index which quantifies image quality degradation between the original image and a filtered image. SSIM is defined in the spatial domain as:

$$SSIM = \frac{2(\mu_x \mu_y + C_1)(\mu_x \mu_y + C_2)}{(\mu_x^2 + m \mu_y^2 + C_1)(\mu_x^2 + \mu_y^2 + C_2)} \quad (5)$$

where in this case x and y are individual images. Preferred results would demonstrate a high SSIM.

E. Segmentation

K-means clustering is an iterative algorithm which attempts to partition observation into k clusters in which each observation belongs to the cluster with the closest mean value. The number of clusters, k is defined, and the distance metric from each observation to the closest mean is quantified using *euclidean distance*. In this algorithm the initial mean values are randomly initialized, and iteratively change until all observation assignments do not change.

F. Segmentation Validation Metrics

To quantify segmentation performance, overlapping metrics such as the *dice similarity coefficient* and *extra fraction* metrics will be used. The DSC is defined as:

1) *Dice Similarity Coefficient*:

$$DSC = \frac{2 * TP}{2 * TP + FP + FN} \quad (6)$$

where TP, FP, and FN are the true positives, false positives, and false negatives respectively. Preferred results should demonstrate high DSC values.

2) *Extra Fraction*: The extra fraction metric is used to define over segmentation and is defined as:

$$EF = \frac{FP}{TP + FN} \quad (7)$$

High extraction fraction values would indicate over segmentation. Therefore, low values for this metric are ideal.

III. EXPERIMENTAL RESULTS

A. Filtering

1) *Gaussian Filter*: As no parameters needed to tuned for the Gaussian filter, the performance of the filter was analyzed with respect to additive noise, and slice thickness. **Figure 2** depicts the filtering validation metrics averaged across all volumes. From the figure, as noise level increases so do

the SNR, PSNR, and SSIM. However, with respect to slice thickness, the filter performs relatively better on thicker slicers when considering SSIM and SNR. However, as slice thickness and noise level increases the PSNR worsens.

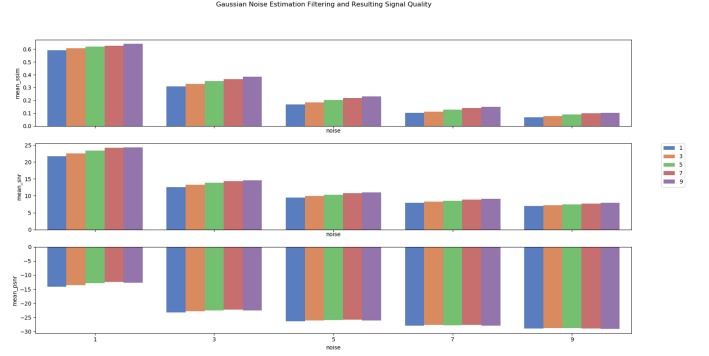


Fig. 2. Gaussian Filter Performance

2) *Median Filter*: The median filter neighbourhood size was optimized with respect to SNR, PSNR, and SSIM. **Figure 3** depicts these validation metrics as a function of neighbourhood size and noise level (%) (indicated in the legend).

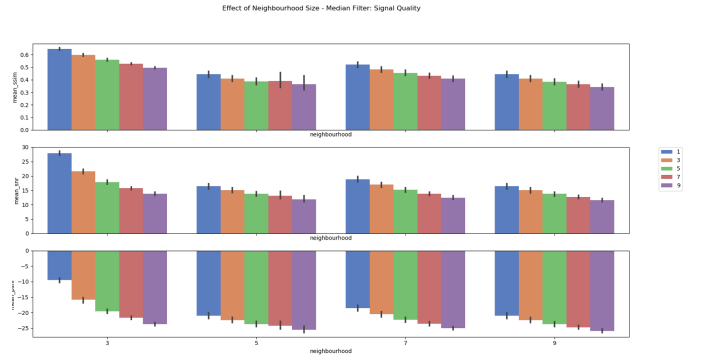


Fig. 3. Median Filter Performance

As neighbourhood size was increased, there was a decrease in SSIM, SNR, and PSNR. This makes sense as a larger neighbourhood would cause more blurring in the resultant image. From the figure, the median filter with a neighbourhood size of 3x3 results on average in images with maintained structured and high SNR and PSNR. As noise level increases, the performance of the median filter decreases as well, as indicated by the decreasing values in SSIM, SNR, and PSNR.

3) *Wiener Filter*: Similar to the median filter, the Wiener filter neighbourhood size was optimized. **Figure 4** depicts the performance of the Wiener filter as a function of neighbourhood size and noise level (%). The results of the Wiener filter echo the results of the median filter, where filter performance decreases with noise level. However, the Wiener filter demonstrates similar SSIM and PSNR results as neighbourhood size increases. As a 3x3 neighbourhood size demonstrates minimally greater performance, this size was chosen when moving forward with segmentation.

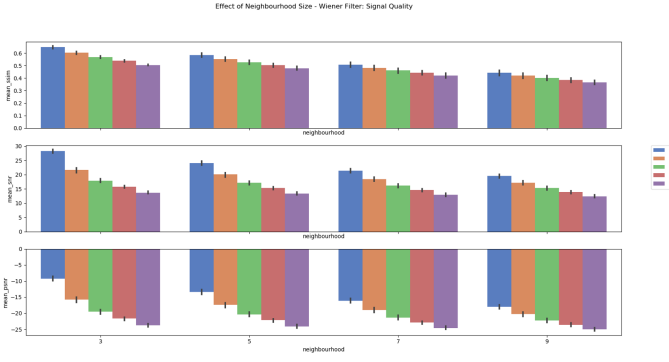


Fig. 4. Wiener Filter Performance

4) *Comparative Performance:* Since the optimal filter parameters were chosen, the filters are compared overall to demonstrate which one quantitatively performs better. In this case, high SSIM, PSNR, and SNR values are desired as each noise level.

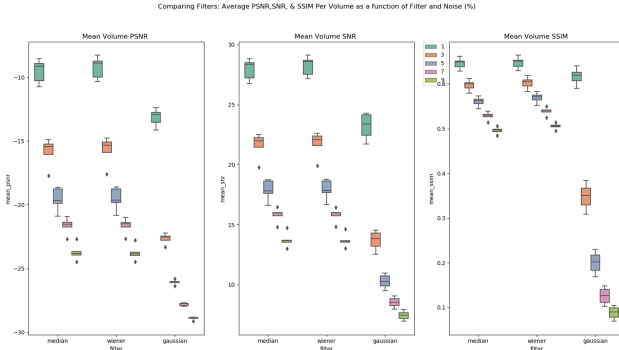


Fig. 5. Comparing All Filters

From **Figure 5**, the median and wiener filter perform fairly similar achieving similar SSIM, SNR, and PSNR distributions at each noise level. In contrast, as noise level increases, the Gaussian filter performance significantly decreases. **Figure 6** depicts qualitative results of the applied filters at a slice thickness of 1mm and noise levels (%) 1, 3, and 7. From **Figure 6**, the median and Wiener filters perform similarly at low and high noise levels for this particular example. In contrast, the Gaussian filter results in over attenuation resulting in blurring where structures become indiscernible. Perhaps the noise estimation method by [5] is not estimating the σ accurately, and therefore results in undesirable filtered images. Based on these results, it is predicted that median and Wiener filtered images would result in similar and good segmentation results, while Gaussian filtered images would result in worsened segmentation.

B. Segmentation

After each volume is filtered, the images are then passed to the k-means clustering segmentation algorithm. The quantitative segmentation results are depicted in **Figure 7**.

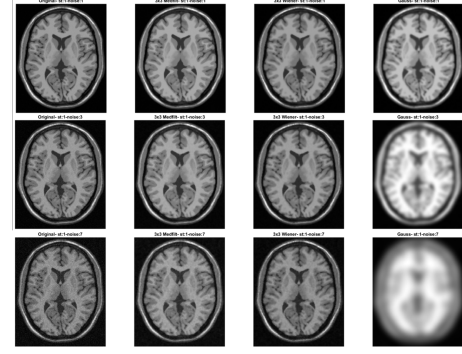


Fig. 6. Comparing All Filters Qualitatively

In general, the Gaussian filter demonstrates the worst segmentation performance across all noise levels and slice thicknesses as indicated by a lower DSC distribution and high EF distribution. With respect to tissue type, the Wiener and median filters seem to have consistent performance, but also has similar performance to images that were not filtered. At increased noise levels, the median filter demonstrates the highest median DSC but does not greatly differ from the Wiener filter. From a different perspective, as slice thickness increases there is similar performance between the original/unfiltered, median, and wiener filtered images. In general, with regards to slice thickness, segmentation performance is better at smaller slice thicknesses. **Figure 8** depicts an example of segmentation for all filters. For this particular example, all filters perform fairly well.

TABLE I
GAUSSIAN FILTER SEGMENTATION RESULTS

Tissue	DSC	EF
White Matter	0.637	0.322
Grey Matter	0.494	inf
CSF	0.668	0.606

TABLE II
MEDIAN FILTER SEGMENTATION RESULTS

Tissue	DSC	EF
White Matter	0.755	0.220
Grey Matter	0.642	inf
CSF	0.777	0.590

TABLE III
WIENER FILTER SEGMENTATION RESULTS

Tissue	DSC	EF
White Matter	0.723	0.290
Grey Matter	0.614	inf
CSF	0.786	0.466

Table I, II, and III demonstrates that across all noise levels and slice thicknesses, the median filter results in the greatest DSC amongst all filters for each tissue type.

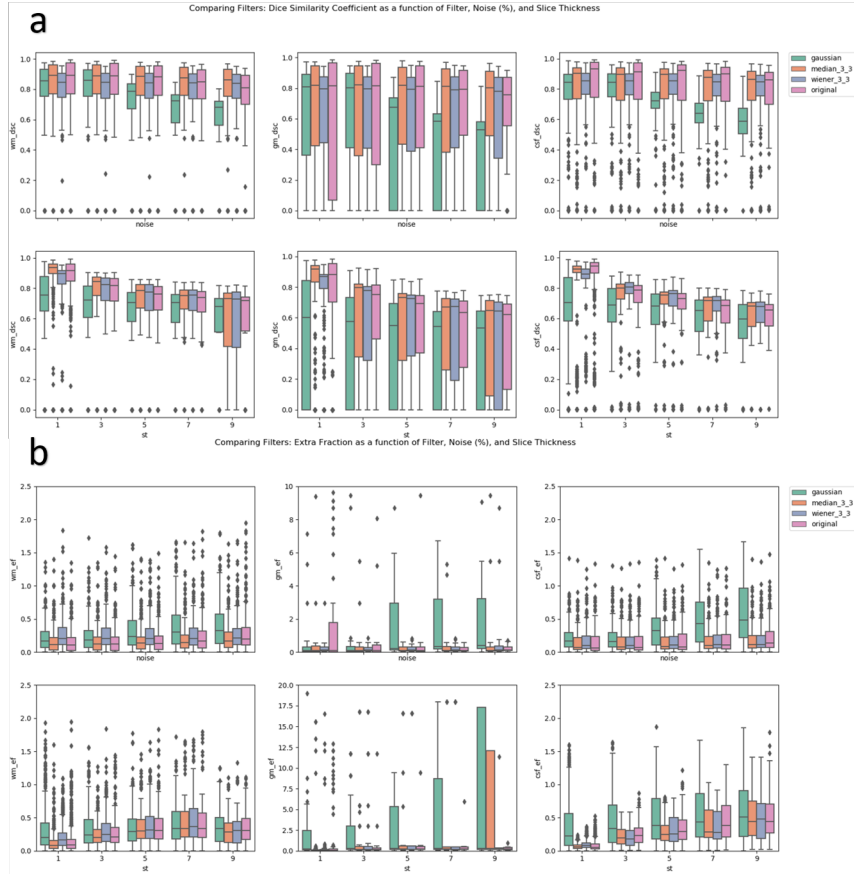


Fig. 7. Segmentation Results - a) Dice Similarity b) Extra Fraction

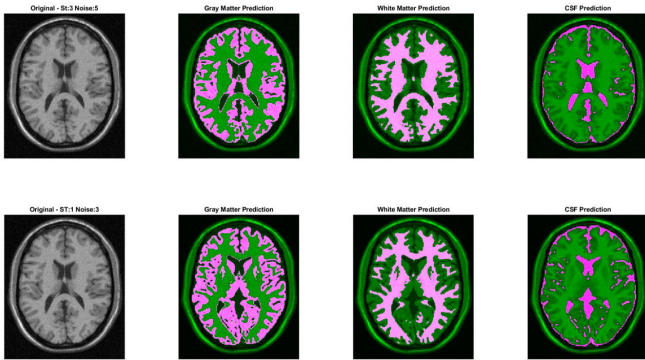


Fig. 8. Segmentation Results Sample Prediction: Pink colour indicates prediction for the respective class

IV. DISCUSSIONS AND CONCLUSIONS

By comparing three different pre-processing filters, their effect on segmentation performance was observed. Overall, the gaussian filter performed the worst on average and resulted in the worst segmentation performance. This is mostly likely due to the inaccuracy when estimating the gaussian parameters. Inaccurate estimation results in over-blurring which would make it difficult for the k-means algorithm to discern tissue

classes. This is especially apparent in segmenting grey matter. Segmentation using Gaussian filtered images resulted in a large range of grey matter DSC values. Even from **Figure 6**, the Gaussian filter actually blends grey and white matter at high noise levels compared to filtered images at low noise levels. Perhaps this is the reason for the low segmentation performance.

Regarding the performance on the median and Wiener filtered images, performance mainly differed as slice thickness increased rather than noise. While there were small differences amongst the filters at different noise levels, there was a consistent decreasing trend in segmentation performance as slice thickness increased (**Figure 7**). This is likely due to the partial volume averaging artefact. This artefact is caused when an imaging voxel contains two different tissues and therefore contains a signal average of the tissue. Furthermore, this artefact results in the loss of contrast between two adjacent tissue in the MR slice image [8], which explains why as slice thickness increased, segmentation performance decreased.

While this paper evaluated the effect of pre-processing techniques on segmentation performance, the paper was limited to single filter pre-processing techniques. For future works, it would be useful to combine filters to achieve better denoising. Furthermore, while k-means clustering demonstrated fair

results, disadvantages of k-means is limited to the number of known classes. By pre-defining class numbers, the algorithm will always segment based on that number regardless if all suspected class types are present. In this application, all tissue classes may not have been present at each layer demonstrating a false poor performance. For future experiments, a more flexible segmentation method should be implemented.

REFERENCES

- [1] A. Alexandra Constantin, B. Ruzena Bajcsy, and C. Sarah Nelson. Unsupervised segmentation of brain tissue in multivariate mri. In *2010 IEEE International Symposium on Biomedical Imaging: From Nano to Macro*, pages 89–92, April 2010.
- [2] J. Grande-Barreto and P. Gómez-Gil. Unsupervised brain tissue segmentation in mri images. In *2018 IEEE International Autumn Meeting on Power, Electronics and Computing (ROPEC)*, pages 1–6, Nov 2018.
- [3] Jing-Hao Xue, Aleksandra Pizurica, Wilfried Philips, Etienne Kerre, Rik Van de Walle, and Ignace Lemahieu. An integrated method of adaptive enhancement for unsupervised segmentation of mri brain images. *Pattern Recognition Letters*, 24:2549–2560, 06 2003.
- [4] Hanafy M. Ali. *MRI Medical Image Denoising by Fundamental Filters*. 2018.
- [5] Shen-Chuan Tai and Shih-Ming Yang. A fast method for image noise estimation using laplacian operator and adaptive edge detection. In *2008 3rd International Symposium on Communications, Control and Signal Processing*, pages 1077–1081, March 2008.
- [6] Rafael C. Gonzalez and Richard E. Woods. *Digital image processing*. Prentice Hall, Upper Saddle River, N.J., 2008.
- [7] Sonka, Vaclav Hlavac. Boyle, Richard. Milan. *Image Processing, Analysis, and Machine Vision*. University Press, 1993.
- [8] Softways. Mri database : Partial volume effect.